Expression of ABCA4 in the retinal pigment epithelium and its implications for Stargardt macular degeneration

Tamara L. Lenis[a], Jane Hu[a], Sze Yin Ng[a], Zhichun Jiang[a], Shanta Sarfare[a,1], Marcia B. Lloyd[a], Nicholas J. Esposito[b], William Samuel[c], Cynthia Jaworski[c], Dean Bok[a,d], Silvia C. Finnemann[b], Monte J. Radeke[e], T. Michael Redmond[c], Gabriel H. Travis[a,f], and Roxana A. Radu[a,2]

[a]Stein Eye Institute, Department of Ophthalmology, David Geffen School of Medicine, University of California, Los Angeles, CA 90095; [b]Department of Biological Sciences, Fordham University, Bronx, NY 10458; [c]Laboratory of Retinal Cell and Molecular Biology, National Eye Institute, National Institutes of Health, Bethesda, MD 20814; [d]Department of Neurobiology, David Geffen School of Medicine, University of California, Los Angeles, CA 90095; [e]Neuroscience Research Institute, University of California, Santa Barbara, CA 93106; and [f]Department of Biological Chemistry, David Geffen School of Medicine, University of California, Los Angeles, CA 90095

Recessive Stargardt disease (STGD1) is an inherited blinding disorder caused by mutations in the *Abca4* gene. ABCA4 is a flippase in photoreceptor outer segments (OS) that translocates retinaldehyde conjugated to phosphatidylethanolamine across OS disc membranes. Loss of ABCA4 in *Abca4*$^{-/-}$ mice and STGD1 patients causes buildup of lipofuscin in the retinal pigment epithelium (RPE) and degeneration of photoreceptors, leading to blindness. No effective treatment currently exists for STGD1. Here we show by several approaches that ABCA4 is additionally expressed in RPE cells. (*i*) By in situ hybridization analysis and by RNA-sequencing analysis, we show the *Abca4* mRNA is expressed in human and mouse RPE cells. (*ii*) By quantitative immunoblotting, we show that the level of ABCA4 protein in homogenates of wild-type mouse RPE is about 1% of the level in neural retina homogenates. (*iii*) ABCA4 immunofluorescence is present in RPE cells of wild-type and *Mertk*$^{-/-}$ but not *Abca4*$^{-/-}$ mouse retina sections, where it colocalizes with endolysosomal proteins. To elucidate the role of ABCA4 in RPE cells, we generated a line of genetically modified mice that express ABCA4 in RPE cells but not in photoreceptors. Mice from this line on the *Abca4*$^{-/-}$ background showed partial rescue of photoreceptor degeneration and decreased lipofuscin accumulation compared with nontransgenic *Abca4*$^{-/-}$ mice. We propose that ABCA4 functions to recycle retinaldehyde released during proteolysis of rhodopsin in RPE endolysosomes following daily phagocytosis of distal photoreceptor OS. ABCA4 deficiency in the RPE may play a role in the pathogenesis of STGD1.

Stargardt disease | retinal pigment epithelium | bisretinoid | lipofuscin | ABCA4

Rhodopsin and the cone-opsin visual pigments are present in the membranous discs of rod and cone outer segments (OS). Upon capture of a photon, the 11-*cis*-retinaldehyde (11cRAL) chromophore coupled to a visual opsin is converted to all-*trans*-retinaldehyde (atRAL), thereby activating the pigment and triggering visual transduction (1). Shortly thereafter, the bleached pigment dissociates, releasing free atRAL into the disc bilayer. Here, retinaldehyde combines rapidly and reversibly with phosphatidylethanolamine (PE) to form *N*-retinylidene-phosphatidylethanolamine (*N*-ret-PE) in the disc membrane. Here, *N*-ret-PE has two potential orientations: with its retinylidene-bearing head group facing into the disc lumen or with the head group facing outward into the cytoplasmic space. The retinol dehydrogenase (RDH8) that reduces atRAL to all-*trans*-retinol (atROL) as a first step in the regeneration of visual chromophore (2) is located in the OS cytoplasm. Cytoplasmically oriented *N*-ret-PE upon dissociation becomes a substrate for RDH8. However, *N*-ret-PE located on the luminal surface is inaccessible by

RDH8. To accelerate the reduction of toxic retinaldehydes, OS membranes contain an ATP-dependent transporter called ABCA4, or ATP-binding cassette subfamily A member 4, that flips *N*-ret-PE from the luminal to cytoplasmic surface of disc membranes (3, 4).

Mutations in the *Abca4* gene are responsible for several inherited blinding diseases including recessive Stargardt macular degeneration (STGD1) and a subset of cone–rod dystrophies (5, 6). STGD1 causes progressive blindness in children and young adults (7). A key pathologic feature of STGD1 is the buildup of fluorescent lipofuscin pigments in retinal pigment epithelium (RPE) cells. The accepted mechanism for bisretinoid formation in the RPE is that, with the loss of ABCA4, the clearance of retinaldehyde released from bleached visual pigments in rod OS is delayed due to the loss of *N*-ret-PE flippase activity. This favors secondary condensation of *N*-ret-PE with another retinaldehyde to form a phospholipid-conjugated bisretinoid such as dihydro-*N*-retinylidene-*N*-retinyl-phosphatidylethanolamine

Significance

Recessive Stargardt macular degeneration (STGD1) and a subset of cone–rod dystrophies are caused by mutations in the *Abca4* gene. The ABCA4 protein is a flippase in photoreceptor cells that helps eliminate retinaldehyde, a toxic photoproduct of vision. Here we found that ABCA4 is additionally present in the retinal pigment epithelium (RPE) of mice at approximately 1% of its abundance in the neural retina. Genetically modified mice that express ABCA4 in RPE but not in photoreceptor cells showed partial rescue of both the lipofuscin accumulation and photoreceptor degeneration observed in *Abca4*$^{-/-}$ mice and in STGD1 patients. These observations suggest that ABCA4 in the RPE prevents photoreceptor degeneration in *Abca4*$^{-/-}$ mice and possibly in STGD1 patients.

[1]Present address: Department of Biomedical Science and Disease, New England College of Optometry, Boston, MA 02115.

[2]To whom correspondence should be addressed. Email: radu@jsei.ucla.edu.

(A2PE-H$_2$) or its oxidized form (A2PE). It is thought that following diurnal phagocytosis of distal photoreceptor OS (8, 9), these bisretinoids are converted to the major lipofuscin fluorophore A2E in the acidic environment of RPE phagolysosomes (10). According to this model, the source of retinaldehyde to form *N*-ret-PE and the various bisretinoids is atRAL released by photobleached rhodopsin and cone opsins in the OS. A strong prediction of this model is that *Abca4*$^{-/-}$ mice reared in total darkness should not accumulate bisretinoids, since photobleaching of visual pigments does not occur in the dark. Unexpectedly, *Abca4*$^{-/-}$ mice maintained in constant darkness accumulated A2E in RPE cells at the same rate as *Abca4*$^{-/-}$ mice reared under 12-h cyclic light (11). This finding suggests that retinaldehyde released by photobleaching of visual pigments is not the major source of bisretinoids that accumulate as lipofuscin in the RPE.

Another possible source of retinaldehyde for A2E formation in the RPE is the 11cRAL chromophore contained within the visual pigments of phagocytosed rod and cone OS discs. The distal 10% of rod and cone OS are diurnally shed and phagocytosed by the RPE (8, 9). Since the dominant ocular retinoid is 11cRAL coupled to rhodopsin, ~10% of visual retinoids are processed daily by the RPE through phagocytosis of photoreceptor OS. This process occurs at similar rates in mice maintained under cyclic light or constant darkness (12). Retinaldehyde released during the degradation of rhodopsin likely condenses with PE on the luminal surface of endolysosome membrane in RPE cells to form *N*-ret-PE. Here, we suggest that ABCA4 performs the same function as in photoreceptor OS: ATP-dependent translocation of *N*-ret-PE from the luminal to cytoplasmic leaflet. This model assumes that ABCA4 is normally present in the endolysosomal membranes of RPE cells. In the current work, we show that ABCA4 is expressed in RPE internal membranes, where it plays a role in preventing the buildup of bisretinoid-containing lipofuscin and preventing photoreceptor degeneration.

Results

The Abca4 Gene Is Expressed in RPE Cells. We used chromogenic in situ hybridization (13) to detect the *Abca4* mRNA in human and wild-type (BALB/c) mouse retina sections. As expected, the *ABCA4* mRNA was intensely expressed in the photoreceptor outer nuclear layer (Fig. 1 *A* and *B*). We also observed significant chromogenic labeling of the *Abca4* mRNA in RPE cells (Fig. 1 *A* and *B*). Importantly, no labeling of photoreceptor nuclei or RPE cells was detected by the same probe in sections of *Abca4*$^{-/-}$ retina (Fig. 1*B*). We also performed in situ hybridization to detect the *ABCA4* mRNA in primary cultured human fetal RPE (hfRPE) cells (14), where we observed robust labeling of the *ABCA4* mRNA (Fig. 1*C*). Positive and negative control probes confirmed tissue-specific chromogenic reactivity by in situ hybridization assay (*SI Appendix*, Fig. S1). Finally, by qRT-PCR we quantified the levels of the *Abca4* mRNAs in 3-wk-old mouse neural retina separated from the RPE/eyecup, normalizing to 18S rRNA. The *Abca4* mRNA level in the wild-type (129/Sv) RPE/eyecup was about 10% of the level in the neural retina sample (*SI Appendix*, Fig. S2).

To confirm the expression of *Abca4* in the RPE, we performed RNA-sequencing (RNA-seq) analysis on RNA extracted from confluent cultures of hfRPE cells. This analysis revealed the presence of *Abca4* and several other RPE-expressed mRNAs including RPE-specific 65-kDa protein (*Rpe65*), Bestrophin-1 (*Best1*), and Lecithin retinol acyltransferase (*Lrat*). As expected, mRNAs for the photoreceptor proteins rhodopsin (*Rho*), melanopsin (*Opn4*), cone M-opsin (*Opn1LW*), and cone S-opsin (*Opn1SW*) were not detected (*SI Appendix*, Table S1). RNA-seq
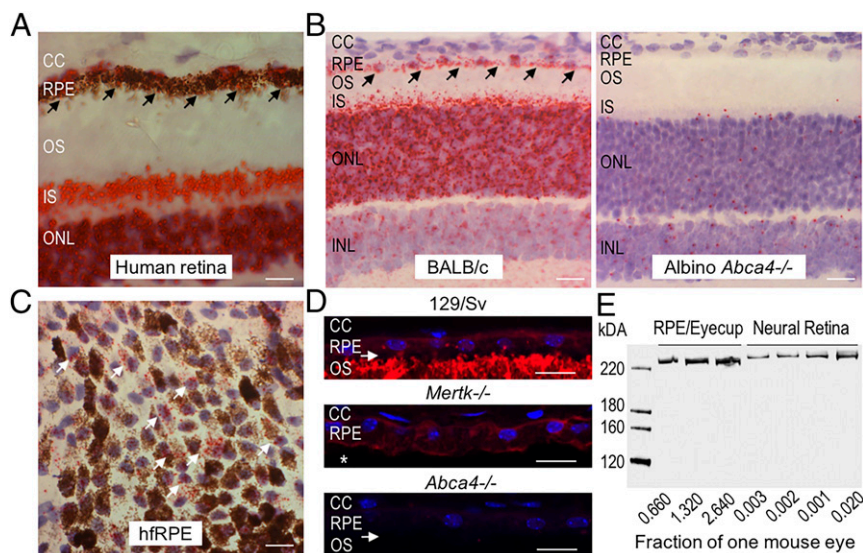

Fig. 1. (*A–C*) *Abca4* mRNA and protein is expressed in RPE cells. In situ hybridization using the RNAscope assay with an *Abca4*-specific probe on human cadaveric ocular sections (*A*), mouse retina sections (*B*), and hfRPE cells in culture (*C*). Note the intense chromogenic reactivity (red punctate staining, indicated by the black arrows) for *Abca4* mRNA in outer nuclear layer (ONL) and inner segments (IS) of the photoreceptor cells and in RPE cells of human (*A*) and wild-type BALB/c sections (*B*, *Left*). This reactivity is absent in *Abca4*$^{-/-}$ tissue (*B*, *Right*). Red punctate staining (white arrows) corresponding to ABCA4 mRNA is also observed in hfRPE cultured cells (*C*). CC, choriocapillaris; INL, inner nuclear layer. (Scale bars, 20 μm.) (*D*) ABCA4 immunohistochemistry (red fluorescence) on retina sections from pigmented wild-type (129/Sv), *Mertk*$^{-/-}$, and *Abca4*$^{-/-}$ mice. Note that ABCA4 immunoreactivity is seen in the RPE and OS of 129/Sv mice and in the RPE but not in the OS (indicated by white asterisk) of *Mertk*$^{-/-}$ mice but is not seen in the retina section from an *Abca4*$^{-/-}$ mouse. The white arrows indicate retinal detachment. Cell nuclei are stained with DAPI (blue). (Scale bars, 10 μm.) (*E*) Representative immunoblots for ABCA4 protein using neural retina and RPE/eyecup homogenates loaded as a fraction of one mouse eye per lane, as indicated. The RNAscope assay (*A–C*) was done with two human cadaveric eyes, three cultured hfRPE cells of different donor eyes, and $n = 3$ mice (5-mo-old) of each genotype; Immunohistochemistry experiments (*D*) were repeated three times with $n = 3$ 5-mo-old mice per group. The immunoblotting experiment (*E*) was done in duplicates varying the fraction of the homogenate corresponding to one mouse eye ($n = 4$ mice for each experiment).

analysis of RPE from fresh bovine eyes also evidenced the *Abca4* mRNA, with greatly reduced or absent expression of mRNAs for photoreceptor-specific proteins (*SI Appendix*, Table S1). These data establish that the *Abca4* gene is expressed in RPE cells.

The ABCA4 Protein Is Present in RPE Internal Membranes. We tested for ABCA4 protein expression in RPE cells by immunofluorescence microscopy. Sections of wild-type (129/Sv) retinas showed ABCA4 immunofluorescence in photoreceptor OS and RPE cells, with much greater immunoreactivity in the OS (Fig. 1D). Mer tyrosine kinase is present in RPE cells and is required for phagocytosis of shed OS discs (15). For this reason, $Mertk^{-/-}$ mice exhibit greatly impaired OS phagocytosis and photoreceptor degeneration, which is complete by 2 mo of age (16). To rule out the possibility that the RPE immunoreactivity is due to ABCA4 in phagocytosed OS discs, we performed immunofluorescence microscopy on retina/RPE sections from 5-mo-old $Mertk^{-/-}$ mice. These sections showed ABCA4 immunoreactivity in RPE cells similar to that in wild-type mice but no OS immunoreactivity (Fig. 1D). The persistence of ABCA4 immunoreactivity in RPE cells from fully degenerated $Mertk^{-/-}$ mice, with no OS immunoreactivity, indicates that ABCA4 is endogenously expressed in RPE. As expected, we observed no ABCA4 immunofluorescence in $Abca4^{-/-}$ retina/RPE sections (Fig. 1D).

To estimate the relative amounts of ABCA4 in OS and RPE, we performed semiquantitative immunoblotting on homogenates of isolated retinas and RPE-containing eyecups from wild-type (129/Sv) mice (Fig. 1E). The amount of protein loaded onto the gel was adjusted to yield similar ABCA4 immunoreactivities in the retina and RPE lanes within the linear range of the infrared-fluorescent scanner used to quantitate the blots. The results of this experiment showed that the total ABCA4 in the RPE is ~1% of the total ABCA4 in the neural retina.

ABCA4 Colocalizes with Endolysosomal Markers. A possible role for ABCA4 in RPE cells, consistent with its known function in photoreceptor OS (3), is as an N-ret-PE flippase that helps clear retinaldehydes released during proteolysis of rhodopsin and cone opsins in phagocytosed OS discs. We tested this possibility by looking for colocalization of ABCA4 with proteins of the endolysosomal system. In retina/RPE sections from wild-type (BALB/c) mice we observed colocalization of ABCA4 with lysosomal-associated membrane protein-1 (LAMP1) in the RPE but not in photoreceptor OS (Fig. 2A). As anticipated, LAMP1 but not ABCA4 immunofluorescence was seen in similar retina sections from $Abca4^{-/-}$ mice (Fig. 2A). ABCA4 also colocalized with the early-endosomal protein Rab5 in RPE cells from wild-type (129/Sv) and $Mertk^{-/-}$ mice (Fig. 2B). The use of $Mertk^{-/-}$ mice here ruled out an OS origin of the ABCA4 in RPE cells. ABCA4 was also present in hfRPE cells, where it exhibited a granular pattern of immunoreactivity consistent with an internal-membrane distribution (Fig. 2C). Here, ABCA4 largely overlapped with caveolin-1 (CAV1) (Fig. 2C), a protein of multiple functions and a marker for RPE phagolysosomes (17). The presence of ABCA4 in hfRPE cells that were never exposed to photoreceptor OS is further evidence that ABCA4 is endogenously expressed in RPE cells. Together, these results suggest that ABCA4 is present in endolysosomal membranes of RPE cells.

Generation of Mice Preferentially Expressing ABCA4 in RPE Cells but Not in Photoreceptors. To study the function of ABCA4 in RPE cells, we prepared a transgene construct containing the mouse *Rpe65* promoter upstream of the *Abca4* coding region. Injection of DNA from this construct into fertilized mouse oocytes yielded several founder lines, only one of which showed significant
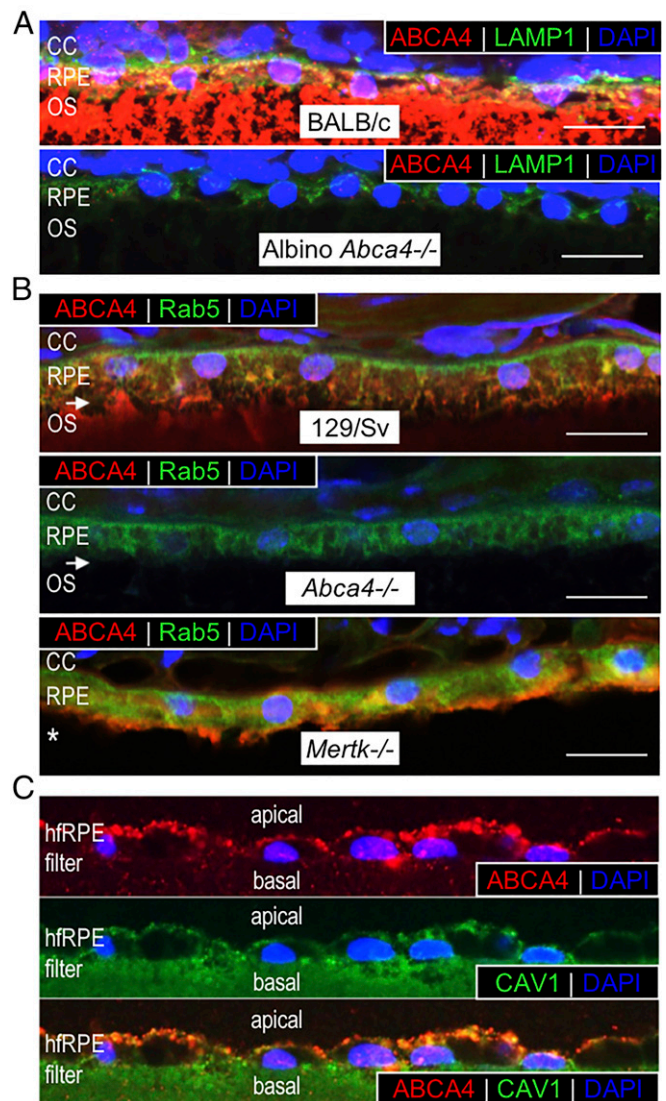

Fig. 2. ABCA4 colocalizes with endolysosomal markers. (A) Representative merged confocal images of retina/RPE sections from 2-mo-old wild-type BALB/c (*Upper*) and albino $Abca4^{-/-}$ (*Lower*) mice reacted with antibodies to ABCA4 (red) and LAMP1 (green). Note that ABCA4 and LAMP1 colocalize in wild-type RPE but not in the OS. LAMP1, but not ABCA4, immunoreactivity is also present in the $Abca4^{-/-}$ RPE cells. (B) Representative merged confocal images of retina sections from 5-mo-old wild-type (129/Sv) (*Top*), $Abca4^{-/-}$ (*Middle*), and $Mertk^{-/-}$ (*Bottom*) mice immunostained with ABCA4 (red) and Rab5 (green) antibodies. Colocalization of ABCA4 and Rab5 is observed in both 129/Sv and $Mertk^{-/-}$ RPE cells as indicated by the orange signal. In the RPE of $Abca4^{-/-}$ retina section only Rab5 immunoreactivity is seen. White arrows indicate retinal detachment, and the white asterisk indicates the absence of OS in the $Mertk^{-/-}$ retina due to photoreceptor degeneration. (C) Representative confocal images of fixed hfRPE cells labeled with ABCA4 (red) (*Top*) or endosomal CAV1 (green) (*Middle*) antibodies. (*Bottom*) Merged confocal images of ABCA4 and CAV1. Note the colocalization of ABCA4 and CAV1. The green labeling of the filter in the CAV1 panel is due to nitrocellulose autofluorescence. Nuclei are stained with DAPI (blue). For murine RPE sections, n = 3 mice per group. For hfRPE cells, each experiment was repeated three times with three different donor cell lines. (Magnification: C, 60×.) (Scale bars, 10 μm.)

ABCA4 expression. We crossed this *RPE-Abca4-Tg*–expressing mouse line onto the albino $Abca4^{-/-}$ background to yield *RPE-Abca4-Tg/Abca4^{-/-}* mice for this study. To compare levels of the ABCA4 protein in retinas and RPE from *RPE-Abca4-Tg/Abca4^{-/-}*, wild-type (BALB/c), and $Abca4^{-/-}$ mice, we performed

quantitative immunoblotting on homogenates from these tissues (Fig. 3A). The levels of ABCA4 in 6-mo-old *RPE-Abca4-Tg/Abca4⁻/⁻* mouse RPE were ~25% of the levels in wild-type RPE, while the levels of ABCA4 protein in retinas from the same mice were negligible (Fig. 3B). Finally, retina sections from 1-y-old wild-type mice showed ABCA4 immunofluorescence in photoreceptor OS and RPE, while sections from age-matched *RPE-Abca4-Tg/Abca4⁻/⁻* mice primarily showed ABCA4 in the RPE. As expected, no ABCA4 immunofluorescence was seen in sections from *Abca4⁻/⁻* mice (Fig. 3C). These data confirm that the *Abca4* transgene is expressed mainly in RPE cells.

Reduced Bisretinoid-Lipofuscin Levels in RPE-Abca4-Tg/Abca4⁻/⁻ Mouse RPE. To determine whether ABCA4 expressed in RPE cells prevents bisretinoid accumulation, we compared levels of several lipofuscin fluorophores in the retina and RPE of 3-mo-old mice (Fig. 4 A–D and SI Appendix, Fig. S3). Levels of A2E (Fig. 4A) were reduced by ~50% in *RPE-Abca4-Tg/Abca4⁻/⁻* vs. *Abca4⁻/⁻* RPE, although the levels of this bisretinoid were still higher in *RPE-Abca4-Tg/Abca4⁻/⁻* than in wild-type RPE. Similarly, levels of atRAL dimer-PE (Fig. 4B), A2PE-H₂ (Fig. 4C), and A2PE (Fig. 4D) were all lower in the RPE of *RPE-Abca4-Tg/Abca4⁻/⁻* mice than in the RPE of *Abca4⁻/⁻* mice. Interestingly, the levels of these bisretinoids were similar in retinas from *RPE-Abca4-Tg/Abca4⁻/⁻* and *Abca4⁻/⁻* mice, as is consistent with the negligible expression of ABCA4 in photoreceptors (Fig. 4 B–D). By confocal microscopy of RPE flat mounts, we observed ~30% lower autofluorescence (488-nm excitation) in the RPE of *RPE-Abca4-Tg/Abca4⁻/⁻* mice than in their *Abca4⁻/⁻* littermates (Fig. 4E and SI Appendix, Fig. S4). Here again, autofluorescence was still greater in *RPE-Abca4-Tg/Abca4⁻/⁻* mice than in wild-type mice. Finally, the fraction of lipofuscin granules per 100 μm² of RPE area was approximately one-half that seen in non-transgenic *Abca4⁻/⁻* littermates (8.6% vs. 15.8%) in electron micrograph sections of RPE (Fig. 4 F and G).

Transgenic Expression of ABCA4 in RPE Slows Photoreceptor Degeneration. An important feature of the *Abca4⁻/⁻* phenotype is the slow degeneration of photoreceptors, which leads to visual loss in STGD1 patients. Here we tested whether transgene-mediated expression of ABCA4 in RPE cells affects the photoreceptor survival rate in *Abca4⁻/⁻* mice by counting photoreceptor nuclei in the outer nuclear layer of retina sections. Compared with wild-type mice, 1-y-old nontransgenic *Abca4⁻/⁻* mice exhibited an ~20% reduction in photoreceptor nuclei (Fig. 5) ($P < 0.0001$). In contrast, *RPE-Abca4-Tg/Abca4⁻/⁻* littermates exhibited only a 10% loss of photoreceptors compared with wild-type mice. Expression of ABCA4 in RPE cells therefore slowed the photoreceptor degeneration seen in *Abca4⁻/⁻* mice by a factor of two.

Discussion

The results presented here establish that ABCA4, known to be present in photoreceptor OS, is also expressed in the RPE. First, we showed that the *Abca4* mRNA is present in mouse, human, and bovine RPE by in situ hybridization (Fig. 1 A–C), RNA-seq (SI Appendix, Table S1), and qRT-PCR analysis (SI Appendix, Fig. S2). These data indicate that the *Abca4* gene is expressed in RPE cells. Next, we showed that the ABCA4 protein is present in RPE cells by quantitative immunoblotting of wild-type mouse retina and RPE homogenates (Fig. 1E) and by immunohistochemistry on wild-type mouse retina/RPE sections (Fig. 1D). To confirm that the ABCA4 protein in RPE cells is endogenously expressed and not due to phagocytosis of ABCA4-containing OS, we demonstrated ABCA4 immunoreactivity in the RPE of 5-mo-old *Mertk⁻/⁻* retina/RPE tissue sections (Fig. 1D). OS
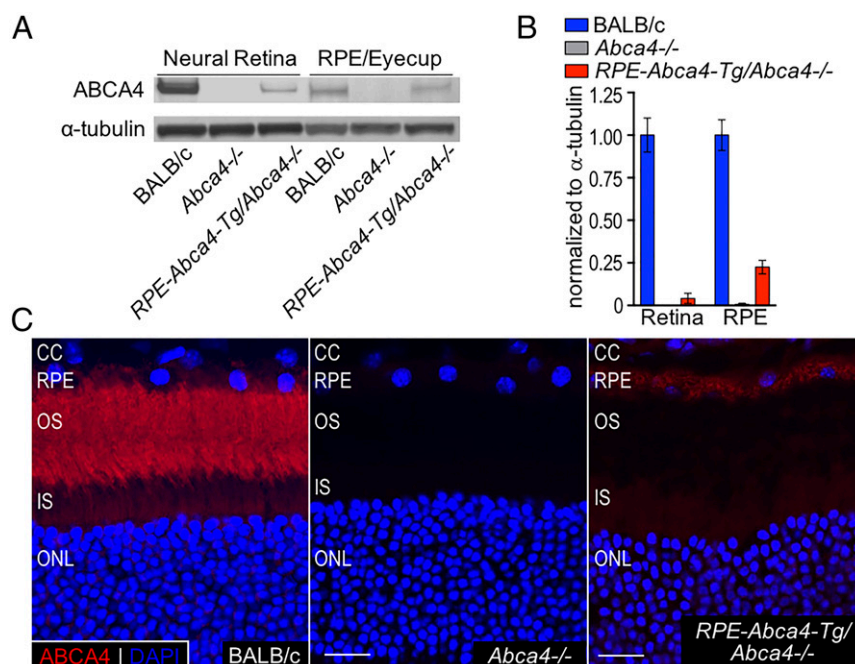

Fig. 3. ABCA4 is expressed in the RPE of *RPE-Abca4-Tg/Abca4⁻/⁻* mice. (A) Representative immunoblots of retina and RPE homogenates from BALB/c, *Abca4⁻/⁻*, and *RPE-Abca4-Tg/Abca4⁻/⁻* mice (all albino) reacted with antisera against ABCA4 or α-tubulin. Total protein load was 10 μg for neural retina and 25 μg for RPE/eyecup homogenates. (B) Levels of ABCA4 protein in *Abca4⁻/⁻* and *RPE-Abca4-Tg/Abca4⁻/⁻* homogenates were normalized to α-tubulin and presented as relative to wild-type BALB/c levels; n = 7 6-mo-old mice per group. (C) Representative confocal images of retinal sections from BALB/c (*Left*), *Abca4⁻/⁻* (*Center*), and *RPE-Abca4-Tg/Abca4⁻/⁻* (*Right*) mice. ABCA4 immunoreactivity (red) in the *RPE-Abca4-Tg/Abca4⁻/⁻* shows specificity mainly for RPE. The OS layer of both *Abca4⁻/⁻* and *RPE-Abca4-Tg/Abca4⁻/⁻* mice is not stained by the ABCA4 antibody. DAPI nuclear staining is shown in blue. (Scale bars, 10 μm.) n = 3 1-y-old mice per group.
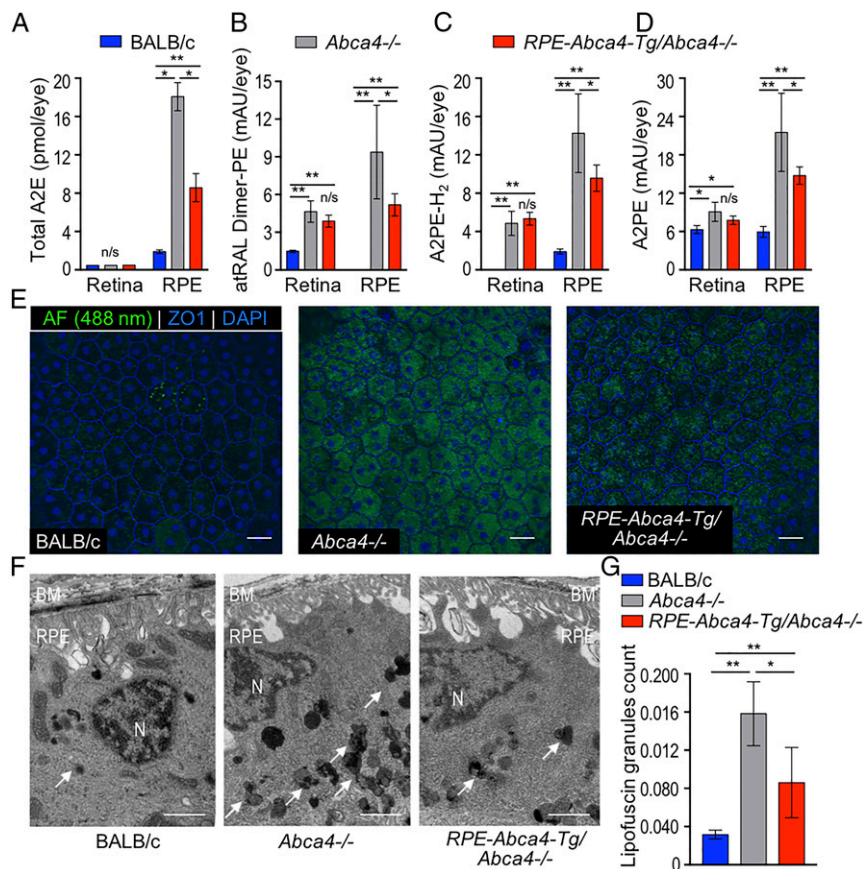
Fig. 4. Bisretinoid, autofluorescence, and lipofuscin levels are reduced in the RPE of *RPE-Abca4-Tg/Abca4*$^{-/-}$ mice. (*A–D*) Bisretinoids were extracted from retina and RPE homogenates of 3-mo-old albino mice and analyzed by normal-phase HPLC. Representative HPLC chromatograms from RPE/eyecup and neural retina extracts are shown in *SI Appendix*, Fig. S3. Note the lower levels of all bisretinoids in RPE from *RPE-Abca4-Tg/Abca4*$^{-/-}$ mice. (*A*) Total A2E (sum of A2E and iso-A2E) is expressed as picomoles per eye. (*B–D*) All-*trans*-retinaldehyde dimer PE (atRAL-Dimer-PE) (*B*), A2PE-H$_2$ (*C*), and A2PE (*D*) are expressed as milliabsorbance units (mAU) per eye. Data are presented as mean ± SD; *n* = 5 mice per group; **P < 0.0001, **P < 0.001; n/s, not significant. (*E*) Representative confocal images of RPE-choroid-sclera flat mounts captured using a 488-nm excitation laser and a 500- to 545-nm emission filter. Note the reduced autofluorescence intensity (AF, green) in the *RPE-Abca4-Tg/Abca4*$^{-/-}$ flat mounts compared with the *Abca4*$^{-/-}$ RPE flat mounts. RPE cell borders are highlighted by anti-ZO1 staining (blue); nuclei are stained with DAPI (blue); *n* = 3 or 4 6-mo-old mice per group. (Scale bars, 20 μm.) (*F*) Representative electron micrographs of RPE cells from 1-y-old BALB/c (*Left*), *Abca4*$^{-/-}$ (*Center*), and *RPE-Abca4-Tg/Abca4*$^{-/-}$ (*Right*) albino mice. Arrows point to polymorphic lipofuscin granules of heterogeneous electron density within RPE cytoplasm. BM, Bruch's membrane; N, nucleus. (Scale bars, 2 μm.) (*G*) Fractional lipofuscin granules per 100-μm^2 cell area were measured and averaged from 10 adjacent electron microscopy images per eye. Data are presented as mean ± SD; *n* = 5–9 mice per group; **P = 0.0186; **P < 0.001.

phagocytosis by RPE cells is blocked in *Mertk*$^{-/-}$ mice, and by age 5 mo the retinas from these mice have lost all photoreceptors (15, 16). Finally, we show that primary cultured hfRPE cells, which were never exposed to ABCA4-containing OS, also express ABCA4 (Fig. 2*C*).

In the RPE, ABCA4 colocalized with three protein markers of the endolysosomal system, LAMP1, Rab5, and CAV1 (Fig. 2). This pattern suggests that ABCA4 is inserted into the membranes of early endosomes where it remains during endolysosomal maturation. In OS disc membranes, ABCA4 has been shown
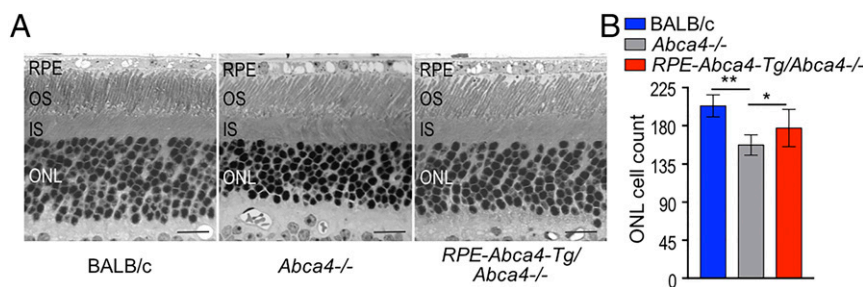

Fig. 5. Photoreceptors are preserved in *RPE-Abca4-Tg/Abca4*$^{-/-}$ vs. *Abca4*$^{-/-}$ mice. (*A*) Representative retina images from 1-y-old albino mice acquired by light microscopy. (Scale bars, 20 μm.) (*B*) Total numbers of photoreceptor nuclei were counted per 100-μm^2 cell area. Note the increased number of cells in the ONL of *RPE-Abca4-Tg/Abca4*$^{-/-}$ mice compared with *Abca4*$^{-/-}$ mice indicating partial rescue of photoreceptor degeneration. Data are presented as mean ± SD; *n* = 5–9 mice per group; *RPE-Abca4-Tg/Abca4*$^{-/-}$ vs. *Abca4*$^{-/-}$, **P = 0.0319; *Abca4*$^{-/-}$ vs. BALB/c, ***P < 0.0001; and *RPE-Abca4-Tg/Abca4*$^{-/-}$ vs. BALB/c, *P = 0.0061.

to translocate *N*-ret-PE from the luminal to the cytoplasmic leaflet (3). The nucleotide-binding domains of ABCA4 are located on the cytoplasmic surface where they have access to cellular ATP. The retinaldehyde reductase RDH8 is also on the cytoplasmic surface where it reduces atRAL to atROL following spontaneous dissociation of *N*-ret-PE. What role does ABCA4 play in RPE cells? Following phagocytosis, the OS disc packet undergoes generalized digestion in the RPE. Retinaldehydes released during proteolysis of rhodopsin and the cone opsins react with PE on the luminal surface of the RPE endolysosomal membrane to form *N*-ret-PE. As shown in Fig. 6, we propose that ABCA4 performs a similar function in RPE cells. RDH11, which reduces atRAL and 11cRAL to their respective retinols (18), is on the cytoplasmic side of the ABCA4-containing membranes in RPE cells, similar to RDH8 in the OS disc membranes. OS contain predominantly 11cRAL as a chromophore in the opsin pigments. However, *N*-ret-PE undergoes both thermal and photoisomerization (19), resulting in a mixture of retinaldehyde isomers. ABCA4 was shown to transport both at- and 11c-*N*-ret-PE (20). A recent study reported elevated bis (monoacylglycero)phosphate lipids in the RPE of *Abca4*$^{-/-}$ mice, suggesting endolysosomal dysfunction in these animals (21). In Fig. 6 we present the pathways in RPE cells for recycling of retinaldehydes in the presence or absence of ABCA4. Experimental systems, such as conditional-knockout mouse and induced pluripotent stem cell (iPSC)-derived RPE cells from Stargardt patients, would be appropriate tools to further validate the proposed model.

By quantitative immunoblotting, we estimate that the abundance of ABCA4 in RPE is ~1% of its abundance in the retina (Fig. 1*E*). Why do photoreceptors require 100-fold more ABCA4 than RPE cells? The cytotoxicity of retinaldehyde is well established (22, 23). The likely role of ABCA4 in photoreceptor OS and RPE cells is to mitigate retinaldehyde toxicity by accelerating its reduction to retinol. The major source of retinaldehyde in photoreceptors is atRAL released following photoactivation of visual pigments. Under daylight conditions the rate of visual pigment activation per photoreceptor can exceed 10^5/s. The great abundance of ABCA4 in rod OS discs is likely an adaptation to clear atRAL at these high rates of production. In contrast, the major source of retinaldehyde in RPE cells is chromophore released by visual pigments undergoing proteolysis in phagolysosomes. Only 10% of OS are phagocytosed per day, and only one retinaldehyde is released per visual pigment during OS digestion. Accordingly, the rate of retinaldehyde production is vastly lower in RPE endolysosomes than in photoreceptor OS. This may explain the lower abundance of ABCA4 in RPE cells. Interestingly, while the ABCA4 protein is present in RPE at only ~1% of its level in the retina (Fig. 1*E*), the *Abca4* mRNA is present in RPE at ~10% of its level in the retina (*SI Appendix*, Fig. S2). This suggests a faster turnover of ABCA4 in the RPE than in the retina, as is consistent with its expression in rapidly turning over endolysosomal membranes. The lower abundance of ABCA4 in the RPE than in the retina does not imply that ABCA4 is less important in the RPE. The observation that A2E accumulates at similar rates in RPE from *Abca4*$^{-/-}$ mice reared under cyclic light or total darkness (11) suggests that de novo bisretinoid formation within RPE endolysosomes contributes more to lipofuscin buildup than do bisretinoids formed in OS discs during light exposure. Therefore, the clearance of retinaldehydes from RPE phagolysosomes may be more critical for photoreceptor viability than for the clearance of retinaldehydes from OS discs.

The phenotype in albino *Abca4*$^{-/-}$ mice includes the accumulation of bisretinoids such as A2E in the RPE, the deposition of fluorescent lipofuscin granules in RPE cells, and slow photoreceptor degeneration (24, 25). To what extent does this phenotype depend on the loss of ABCA4 from RPE cells? We addressed this question by expressing ABCA4 in the RPE of transgenic *Abca4*$^{-/-}$ mice. These *RPE-Abca4-Tg/Abca4*$^{-/-}$ mice expressed the ABCA4 protein in the RPE at ~25% of the level in wild-type RPE (Fig. 3*B*). Although retina homogenates from these mice showed a weak band by ABCA4 immunoblotting (Fig. 3*A*), we observed no labeling of photoreceptor OS by ABCA4 immunohistochemistry (Fig. 3*C*). This band in retina homogenates probably reflects contamination of the retina with ABCA4-expressing RPE during dissection or ectopically expressed ABCA4 in nonphotoreceptor cells of the retina. ABCA4 expression in the retina is therefore an unlikely factor in the rescue of the *Abca4*$^{-/-}$ phenotype *RPE-Abca4-Tg/Abca4*$^{-/-}$ mice. Despite the expression of ABCA4 in the RPE at only ~25% of wild-type RPE expression, we observed an ~50% reduction of A2E accumulation in *RPE-Abca4-Tg/Abca4*$^{-/-}$ vs. nontransgenic *Abca4*$^{-/-}$ mouse RPE (Fig. 4*A*). We also observed an ~50% slowing of photoreceptor degeneration in *RPE-Abca4-Tg/Abca4*$^{-/-}$ vs. nontransgenic *Abca4*$^{-/-}$ mice (Fig. 5). Thus, expression of ABCA4 in RPE cells at ~25% of the
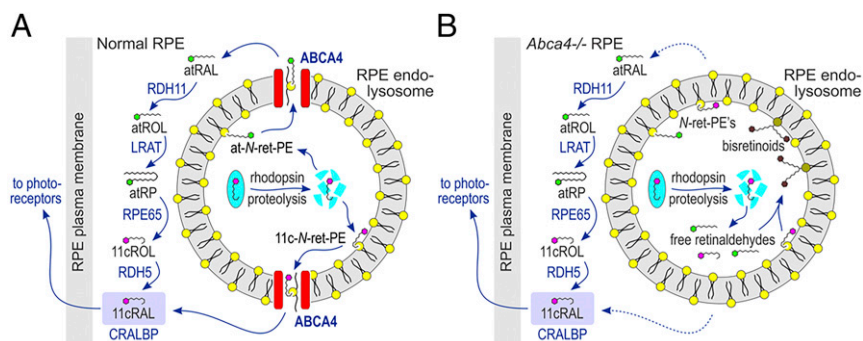

Fig. 6. Proposed function of ABCA4 in the endolysosomal membranes of RPE. (*A*) Normal RPE cell. 11cRAL released during proteolysis of rhodopsin within a phagolysosome condenses with PE on the luminal surface to form 11-*cis*-*N*-retinylidene-phosphatidylethanolamine (11c-*N*-ret-PE), which undergoes isomerization to form a mixture of all-*trans* (at) and 11c-*N*-ret-PEs. Both *N*-ret-PE isomers are flipped by ABCA4 to the cytoplasmic surface, where hydrolysis of *N*-ret-PE is driven by mass action through binding of 11cRAL by cellular retinaldehyde-binding protein (CRALBP) or the reduction of atRAL to atROL by retinol dehydrogenase type 11 (RDH11). The atROL is processed by the RPE visual cycle through esterification by lecithin retinol acyltransferase (LRAT) to yield an all-*trans*-retinyl ester such as all-*trans*-retinyl palmitate (atRP), isomerization by RPE65 to yield 11-*cis*-retinol (11cROL), and oxidation by retinol dehydrogenase type 5 (RDH5) to yield 11cRAL, which binds to CRALBP. 11cRAL leaves the RPE cell to regenerate visual pigments in the adjacent photoreceptor OS. (*B*) *Abca4*$^{-/-}$ mutant RPE cell. The lack of ABCA4 in RPE endolysosomes of *Abca4*$^{-/-}$ mice or STGD1 patients causes delayed clearance of retinaldehydes and hence higher concentrations of both free retinaldehydes and *N*-ret-PE. This leads to secondary condensation of atRAL or 11cRAL with *N*-ret-PE to form bisretinoids.

level in wild-type mice yielded ~50% rescue of both lipofuscin accumulation and photoreceptor degeneration. Expression of ABCA4 in the RPE at the wild-type level may deliver greater and possibly complete rescue of RPE lipofuscin accumulation and photoreceptor degeneration.

Interestingly, atRAL-dimer and the phospholipid-conjugated bis-retinoids A2PE-H$_2$ and A2PE were present at approximately equal levels in retinas from *RPE-Abca4-Tg/Abca4*$^{-/-}$ and nontransgenic *Abca4*$^{-/-}$ mice (Fig. 4 *B–D*). Thus, the formation of these retinaldehyde condensation products in the retina was unaffected by transgenic expression of ABCA4 in the RPE and may have formed due to the loss of ABCA4 in photoreceptor OS. These observations are further evidence of negligible ABCA4 expression in photoreceptors of *RPE-Abca4-Tg/Abca4*$^{-/-}$ mice.

The findings presented here have implications for the treatment of *Abca4*-dependent retinopathies. One treatment approach is gene therapy. If ABCA4 were expressed only in photoreceptor OS, as previously thought, treatment would require efficient transduction of photoreceptors by a recombinant virus containing the 6.8-kb *Abca4* coding region. However, photoreceptors are transduced at lower efficiency than RPE cells (26). Thus, RPE cells are more tractable than photoreceptors as targets for gene therapy of *Abca4*-mediated diseases (27). The best strategy for gene therapy of patients with *Abca4*-dependent retinopathies may be to target both RPE cells and photoreceptors. A second treatment approach is cell transplantation. Here, again, expression of ABCA4 in RPE cells opens therapeutic possibilities. The *Abca4* gene defects could be corrected by targeted gene editing in iPSCs derived from a STGD1 patient's fibroblasts. These cells could then be programed to become functional RPE cells. Numerous studies have shown successful transplantation of iPSC-derived RPE cells into the subretinal space of animals and humans (28, 29).

In summary, we have shown that ABCA4 is expressed in RPE cells and that at least part of the ocular *Abca4*$^{-/-}$ phenotype is caused by the loss of RPE-expressed ABCA4. These observations suggest that RPE cells, in addition to the photoreceptors, should be targeted in rescue approaches to treat *Abca4*-mediated retinal degenerations.

Methods

Animals. All experiments were performed in accordance with the Association for Research in Vision and Ophthalmology Statement for the Use of Animals in Ophthalmic and Vision Research and University of California, Los Angeles Institutional Animal Care and Use Committee guidelines. Animals were housed in normal cyclic 12-h light/12-h dark conditions and were fed ad libitum. Pigmented wild-type (129/Sv), *Mertk*$^{-/-}$ mice (backcrossed at least five times onto 129/Sv) and *Abca4*$^{-/-}$ mice were used for ABCA4 protein-localization studies. Albino wild-type (BALB/c) mice and *Abca4*$^{-/-}$ mice (on the BALB/c background) were used for in situ hybridization studies. Transgenic mice expressing *Abca4* in the RPE on the albino *Abca4*$^{-/-}$ background (*RPE-Abca4-Tg/Abca4*$^{-/-}$) were compared with nontransgenic *Abca4*$^{-/-}$ littermate controls and BALB/c mice for all other studies. All animals were homozygous for the *Rpe65* Leu450 variant and were free of the *rd8* mutation in the Crumbs homolog-1 gene.

Generation of the RPE-Abca4-Tg/Abca4$^{-/-}$ **Transgene.** We generated a transgenic construct (*SI Appendix*, Fig. S5) containing the normal mouse *Abca4* coding region downstream of the RPE-specific *Rpe65* promoter. Briefly, a 700-bp fragment of the *Rpe65* gene containing the promoter, 5′ UTR, and first intron was amplified from pTR4 plasmid and subcloned into the HindIII (5′) and PstI (3′) restriction sites of the pSTEC-1 vector (30, 31). The *Rpe65* promoter/intron 1 complex was then subcloned into the 5′ end of the *Abca4* cDNA in the pSport-*Abca4* plasmid using EcoRI (5′) and SalI (3′) restriction sites. The entire transgene (*Rpe65-Abca4*) was excised from the pSport6-*Abca4* by EcoRI restriction. The construct was sent to the University of California, Los Angeles Transgenic Core facility for fertilized oocyte injection, which resulted in six lines of transgenic mice. Each line was crossed onto the albino *Abca4*$^{-/-}$ background, and one line was identified as having the most robust RPE-specific expression of ABCA4 by qRT-PCR, immunoblotting, and

immunocytochemistry. Primers used for genotyping *RPE-Abca4-Tg/Abca4*$^{-/-}$ mice were (forward) AGG AAA AGG CAG AAG ATT CGC TTT GTA G and (reverse) TGG GAA AAT GGC ATT CAT GCT GAC.

In Situ Hybridization. Retina sections of eyes from a 52-y-old human donor (generous gift of Gregory Hageman, University of Utah, Salt Lake City); and 84-y-old human eyes (San Diego Eye Bank), human fetal RPE (hfRPE) cultured cells (2 to 6 wk in culture), and eyes from 3-mo-old mice were used for in situ hybridization studies. Prior consent was obtained for using the postmortem human donor eyes samples, and the research adhered to the tenets of the Declaration of Helsinki. The assays were done with the RNAscope 2.5 HD Chromogenic Detection Kit (Advanced Cell Diagnostics) according to the manufacturer's protocol. Tissues were hybridized with target oligo probes (Advanced Cell Diagnostics) for murine or human ABCA4, murine or human RNA polymerase II subunit A probe (Polr2A) as a positive control probe, or bacterial dihydrodipicolinate reductase as a negative control probe, followed by amplification steps and chromogenic detection with Fast Red (Advance Cell Diagnostics). Images were collected with a Zeiss Axiophot microscope fitted with a 40× oil-immersion objective lens and a CoolSNAP digital camera (Media Cybernetics). Detailed methods are provided in *SI Appendix*.

RPE Cell-Culture Immunocytochemistry. A comprehensive protocol for culture of hfRPE cells has been previously described (14). After 2 mo in culture, hfRPE cells with their associated filters were fixed in 4% formaldehyde/0.1 M phosphate buffer, embedded in agarose (Type XI low gelling temperature; Sigma-Aldrich), and cut into 100-μm sections on a VT1000S vibratome (Leica Microsystems). The sections were blocked with goat or donkey serum and 1% BSA in 1× PBS followed by separate incubation with rabbit anti-ABCA4 (1:100; ab72955; Abcam) and goat anti-caveolin1 (1:100; ab36152; Abcam). The sections were rinsed and incubated in secondary antibodies conjugated with Alexa Fluor dyes (goat anti-rabbit IgG-647 or donkey anti-goat IgG-594; 1:500; Invitrogen). The sections were stained with DAPI nuclear marker (Invitrogen), mounted with 5% n-propyl gallate in 100% glycerol, and imaged with an Olympus FluoView FV1000 confocal microscope under a 60× oil-immersion objective lens.

Mouse Tissue Immunohistochemistry. Mice under deep isoflurane-induced anesthesia were perfused and fixed in 4% paraformaldehyde/0.1 M sodium phosphate buffer. Eyes were enucleated and immersed in the same fixative overnight after preparation of eyecups and then were infiltrated with 10–30% sucrose for cryoprotection. Eyecups were embedded in cryo-Optimal Cutting Temperature embedding medium (OCT; Tissue-Tek) and cut into 10-μm sections. Slides for colocalization studies were blocked with normal goat serum and 1% BSA and were probed overnight at 4 °C with rabbit polyclonal anti-ABCA4 (1:100; ab72955; Abcam), mouse monoclonal anti-Rab5 (1:75; sc-46692; Santa Cruz), and mouse anti-LAMP1 (1:100; ab25630; Abcam) primary antibodies. Slides for ABCA4 expression in albino and transgenic mice were probed with mouse monoclonal anti-ABCA4 [1:1,000; generous gift from Hui Sun (University of California, Los Angeles) and Robert S. Molday (University of British Columbia, Vancouver) (32)] in conjunction with the Mouse-on-Mouse Immunodetection Kit (Vector Labs). Retina sections from pigmented mice were bleached for 30 s using the Melanin Bleach Kit (Polysciences); bleaching was quenched with 50 mM ammonium chloride for 25 min, and sections were washed, and blocked with 1% BSA and 5% goat serum before probing with rabbit polyclonal anti-ABCA4 primary antibody (1:100; Abcam). All sections were washed and labeled with secondary antibodies conjugated Alexa Fluor 647 (1:500; Invitrogen) or DyLight 647 streptavidin (1:150; Vector Labs) for 1 h at RT. Images were obtained with an Olympus FluoView FV1000 confocal microscope as above.

Immunoblotting. Five-month-old mouse eyes were harvested, and the neural retina was separated from the RPE (eyecup containing RPE/Bruch's membrane/choroid) and homogenized in 1× PBS with Halt Protease Inhibitor mixture (Life Technologies). Protein samples were treated with Benzonase nuclease (Sigma-Aldrich) at RT for 1 h and were rehomogenized with 0.5–1% SDS, followed by centrifugation (3,000 × g for 10 min) to collect the supernatant. Protein concentrations were measured using the Micro BCA Protein Assay Kit (Thermo Fisher), and samples were fractionated on 4–12% Bis-Tris gels (Invitrogen). Membranes were blocked with Odyssey blocking buffer (LI-COR Biosciences) followed by incubation in primary antibody overnight at 4 °C [goat anti-ABCA4 (1:200; sc-21460; Santa Cruz), goat anti-ABCA4 (1:500; EB08615; Everest Biotech Ltd.), and mouse anti–α-tubulin (1:1,000; T9026; Sigma-Aldrich)]. Membranes were washed with PBS-Tween,

probed for 1 h at RT with cognate IR-dye–labeled secondary antibodies from LI-COR, and imaged with the CLx Odyssey system (LI-COR). Band intensity corresponding to a known homogenate fraction was determined using the LI-COR application.

Quantitation of A2E in Mouse Eyes. Bisretinoids were extracted by chloroform followed by analysis using HPLC as described previously (33). Briefly, retina and RPE samples were homogenized in 1× PBS, washed with chloroform/methanol (2:1, vol/vol), and extracted with chloroform (4:3, vol/vol). The organic phase was isolated after centrifugation at $1,000 \times g$ for 10 min, dried under argon, and resuspended in 100 μL of isopropanol. Absorbance units corresponding to the A2E and iso-A2E peaks at 435 nm were converted to picomoles using a calibration curve with authentic standards and published molar extinction coefficient (34).

RPE Flat Mount. Eyes of 6-mo-old mice were enucleated, fixed in 2% paraformaldehyde/0.1 M sodium phosphate buffer (NaPO$_4$, pH 7.4) for 30 min at RT, and rinsed and dissected in 0.1 M NaPO$_4$, removing the neurosensory retina and anterior segment to create RPE-choroid-scleral eyecups. To flatten the eyecups, eight leaflets were made with straight cuts using microdissection scissors. The resultant RPE-choroid-scleral flat mounts were permeabilized with 1% Triton X-100, blocked with 1% BSA/5% goat serum, and incubated at 4 °C overnight with rabbit anti-ZO1 (1:100; Thermo Fisher), mounted with ProLong Gold antifade with DAPI (Life Technologies), and imaged with the Olympus FV 1000 confocal microscope (60× objective). Autofluorescence was detected by excitation with a 488-nm (argon) laser with a 500- to 545-nm emission filter, and images were quantified using the ImageJ program (NIH) (35).

Light and Electron Microscopy. Light and electron microscopy analyses were done as previously described (36). The total number of photoreceptor nuclei in three adjacent midperipheral visual field locations per eye were averaged and plotted in Microsoft Excel (n = 5–9 animals per group). The fractional lipofuscin granules were measured by obtaining the area (in square micrometers) occupied by lipofuscin over the area (in square micrometers) occupied by cytoplasm. Each animal's fractional lipofuscin granule measurement corresponded to an average of at least 10 adjacent electron microscopy images from one eye (n = 5–9 animals per group). Detailed methods are provided in *SI Appendix*.

Statistical Analysis. The results are presented as means with SD of a minimum of four to six animals per group unless otherwise specified. Two-group comparisons were performed with Student's t testing using Microsoft Excel; multiple-group comparisons were performed using one-way ANOVA testing with Tukey–Kramer post hoc analyses using JMP Pro12.0 (SAS).

1. Wald G (1968) Molecular basis of visual excitation. *Science* 162:230–239.
2. Rattner A, Smallwood PM, Nathans J (2000) Identification and characterization of all-trans-retinol dehydrogenase from photoreceptor outer segments, the visual cycle enzyme that reduces all-trans-retinal to all-trans-retinol. *J Biol Chem* 275:11034–11043.
3. Quazi F, Lenevich S, Molday RS (2012) ABCA4 is an N-retinylidene-phosphatidylethanolamine and phosphatidylethanolamine importer. *Nat Commun* 3:925.
4. Sun H, Nathans J (1997) Stargardt's ABCR is localized to the disc membrane of retinal rod outer segments. *Nat Genet* 17:15–16.
5. Allikmets R (1997) A photoreceptor cell-specific ATP-binding transporter gene (ABCR) is mutated in recessive Stargardt macular dystrophy. *Nat Genet* 17:122.
6. Maugeri A, et al. (2000) Mutations in the ABCA4 (ABCR) gene are the major cause of autosomal recessive cone-rod dystrophy. *Am J Hum Genet* 67:960–966.
7. Burke TR, et al. (2014) Quantitative fundus autofluorescence in recessive Stargardt disease. *Invest Ophthalmol Vis Sci* 55:2841–2852.
8. Young RW, Bok D (1969) Participation of the retinal pigment epithelium in the rod outer segment renewal process. *J Cell Biol* 42:392–403.
9. Young RW, Bok D (1970) Autoradiographic studies on the metabolism of the retinal pigment epithelium. *Invest Ophthalmol* 9:524–536.
10. Mata NL, Weng J, Travis GH (2000) Biosynthesis of a major lipofuscin fluorophore in mice and humans with ABCR-mediated retinal and macular degeneration. *Proc Natl Acad Sci USA* 97:7154–7159.
11. Boyer NP, et al. (2012) Lipofuscin and N-retinylidene-N-retinylethanolamine (A2E) accumulate in retinal pigment epithelium in absence of light exposure: Their origin is 11-cis-retinal. *J Biol Chem* 287:22276–22286.
12. LaVail MM (1976) Rod outer segment disk shedding in rat retina: Relationship to cyclic lighting. *Science* 194:1071–1074.
13. Stempel AJ, Morgans CW, Stout JT, Appukuttan B (2014) Simultaneous visualization and cell-specific confirmation of RNA and protein in the mouse retina. *Mol Vis* 20:1366–1373.
14. Hu J, Bok D (2010) Culture of highly differentiated human retinal pigment epithelium for analysis of the polarized uptake, processing, and secretion of retinoids. *Methods Mol Biol* 652:55–73.
15. Feng W, Yasumura D, Matthes MT, LaVail MM, Vollrath D (2002) Mertk triggers uptake of photoreceptor outer segments during phagocytosis by cultured retinal pigment epithelial cells. *J Biol Chem* 277:17016–17022.
16. Duncan JL, et al. (2003) An RCS-like retinal dystrophy phenotype in mer knockout mice. *Invest Ophthalmol Vis Sci* 44:826–838.
17. Sethna S, et al. (2016) Regulation of phagolysosomal digestion by caveolin-1 of the retinal pigment epithelium is essential for vision. *J Biol Chem* 291:6494–6506.
18. Haeseleer F, et al. (2002) Dual-substrate specificity short chain retinol dehydrogenases from the vertebrate retina. *J Biol Chem* 277:45537–45546.
19. Kaylor JJ, et al. (2017) Blue light regenerates functional visual pigments in mammals through a retinyl-phospholipid intermediate. *Nat Commun* 8:16.
20. Quazi F, Molday RS (2014) ATP-binding cassette transporter ABCA4 and chemical isomerization protect photoreceptor cells from the toxic accumulation of excess 11-cis-retinal. *Proc Natl Acad Sci USA* 111:5024–5029.
21. Anderson DMG, et al. (2017) Bis(monoacylglycero)phosphate lipids in the retinal pigment epithelium implicate lysosomal/endosomal dysfunction in a model of Stargardt disease and human retinas. *Sci Rep* 7:17352.
22. Chen C, Thompson DA, Koutalos Y (2012) Reduction of all-trans-retinal in vertebrate rod photoreceptors requires the combined action of RDH8 and RDH12. *J Biol Chem* 287:24662–24670.
23. Harper WS, Gaillard ER (2001) Studies of all-trans-retinal as a photooxidizing agent. *Photochem Photobiol* 73:71–76.
24. Radu RA, et al. (2008) Accelerated accumulation of lipofuscin pigments in the RPE of a mouse model for ABCA4-mediated retinal dystrophies following Vitamin A supplementation. *Invest Ophthalmol Vis Sci* 49:3821–3829.
25. Weng J, et al. (1999) Insights into the function of Rim protein in photoreceptors and etiology of Stargardt's disease from the phenotype in abcr knockout mice. *Cell* 98:13–23.
26. Calame M, et al. (2011) Retinal degeneration progression changes lentiviral vector cell targeting in the retina. *PLoS One* 6:e23782.
27. Natkunarajah M, et al. (2008) Assessment of ocular transduction using single-stranded and self-complementary recombinant adeno-associated virus serotype 2/8. *Gene Ther* 15:463–467.
28. Carr AJ, et al. (2009) Protective effects of human iPS-derived retinal pigment epithelium cell transplantation in the retinal dystrophic rat. *PLoS One* 4:e8152.
29. Schwartz SD, et al. (2015) Human embryonic stem cell-derived retinal pigment epithelium in patients with age-related macular degeneration and Stargardt's macular dystrophy: Follow-up of two open-label phase 1/2 studies. *Lancet* 385:509–516.
30. Boulanger A, Liu S, Henningsgaard AA, Yu S, Redmond TM (2000) The upstream region of the Rpe65 gene confers retinal pigment epithelium-specific expression in vivo and in vitro and contains critical octamer and E-box binding sites. *J Biol Chem* 275:31274–31282.
31. Stec DE, Morimoto S, Sigmund CD (2001) Vectors for high-level expression of cDNAs controlled by tissue-specific promoters in transgenic mice. *Biotechniques* 31:256–258, 260.
32. Illing M, Molday LL, Molday RS (1997) The 220-kDa rim protein of retinal rod outer segments is a member of the ABC transporter superfamily. *J Biol Chem* 272:10303–10310.
33. Radu RA, et al. (2011) Complement system dysregulation and inflammation in the retinal pigment epithelium of a mouse model for Stargardt macular degeneration. *J Biol Chem* 286:18593–18601.
34. Parish CA, Hashimoto M, Nakanishi K, Dillon J, Sparrow J (1998) Isolation and one-step preparation of A2E and iso-A2E, fluorophores from human retinal pigment epithelium. *Proc Natl Acad Sci USA* 95:14609–14613.
35. Schneider CA, Rasband WS, Eliceiri KW (2012) NIH image to ImageJ: 25 years of image analysis. *Nat Methods* 9:671–675.
36. Lenis TL, et al. (2017) Complement modulation in the retinal pigment epithelium rescues photoreceptor degeneration in a mouse model of Stargardt disease. *Proc Natl Acad Sci USA* 114:3987–3992.

MEDICAL SCIENCES